

## THE EFFECT OF PUMPING WATER FROM WELLS IN AN AQUIFER

**K. G. Warui<sup>1</sup>, G.X. Stower<sup>2</sup>, J. K. Sigey<sup>3</sup>**

<sup>1</sup>Mombasa Polytechnic University College, Mombasa, Kenya

<sup>2</sup>Kenyatta University, Nairobi Kenya

<sup>3</sup>Jomo Kenyatta University of Agriculture and Technology, Nairobi Kenya

Email: kennwarui@gmail.com

### Abstract

Groundwater is sensitive to the climate change and agricultural activities in arid and semi-arid areas. Over the past several decades, human activities, such as groundwater extraction for irrigation, have resulted in aquifer overdraft and disrupted the natural equilibrium in these areas. This study reports research on the effect of pumping water from several wells in a given aquifer. We have considered, for simplicity, an idealized one layer aquifer which has been discretized into 49 identical blocks studied on the middle horizontal row of blocks. We have developed a numerical simulating model by discretizing the equation of continuity which we have converted into computer codes. A program has then been written. This program has successfully generated both hydraulic head and velocity profile distributions. The results reveal that there are less hydraulic head losses on pumpage from blocks which are far apart, the velocities being least in blocks which are far from the pumpage blocks. The results obtained have a high correlation with those from the well-known Theis equation for drawdown. The results would greatly help in limiting the usage of a given aquifer with respect to the maximum number of wells permissible in the aquifer as well as predict the levels of groundwater in a particular aquifer.

**Key words:** Aquifer, piezometric height, velocity profiles and simulation

## 1.0 Introduction

### 1.1 Literature review

Groundwater is often called the forgotten resource. Raudkivi and Callander (1976) define it as all interstitial water below the water table, however deep down it may occur. It lies beneath our feet and supplies wells, bores, springs and flows to our rivers. Groundwater as a source of public water supply has attained considerable importance as a result of its large volume (97%) of occurrence irrespective of climatic conditions. According from The Environment Agency (May, 2012), one third of the water utilized in England, for instance, comes from groundwater. Globally, one third of the world's population is dependent upon groundwater (Evans, 2006). In terms of quality, groundwater is usually low in organic and anthropogeneous pollution except in areas of shallow course aquifers (Ako, 1996).

Groundwater is contained in porous media with substantial quantities found in geologic formations called aquifers. Withdrawal of ground water by pumping is the most significant human activity that alters the amount of groundwater in storage and the rate of discharge from an aquifer. Excessive groundwater level declines have been known to produce serious ecological problems, such as land desertification and soil salinization, displacing inhabitants from their ancestral homeland (Shaoyuan, 2010).

The removal of water stored in geologic materials near the well sets up hydraulic gradients that induce flow from more distant regions of the aquifer. As groundwater storage is depleted within the radius of influence of pumping, water levels in the aquifer decline. The area of water level decline is called the cone of depression, and its size is controlled by the rate and duration of pumping, the storage characteristics of the aquifer, and the ease with which water is transmitted through the geologic materials to the well. The development of a cone of depression can result in an overall decline in water levels of a large geographic area, change the direction of groundwater flow within an aquifer, reduce the amount of base flow to streams, and capture water from a stream or from adjacent aquifers. In areas having a high density of pumped wells, multiple cones of depression can develop within an aquifer (US Geological Survey, 2005). Consequently, it has become extremely important to accurately simulate and predict potential groundwater level changes in these regions so that appropriate water resources management and environmental protection policies can be developed and implemented (Huo *et al.*, 2005).

Due to relative inaccessibility of the aquifers (Napie, 1983), slow pace of subsurface processes and high expenses involved in performing actual ground water experiments, numerical simulation modeling has been found to be one of the most effective techniques of studying ground water flow process (Davis, 1986; Zhao *et al.*, 2005; Matej *et al.*, 2007).

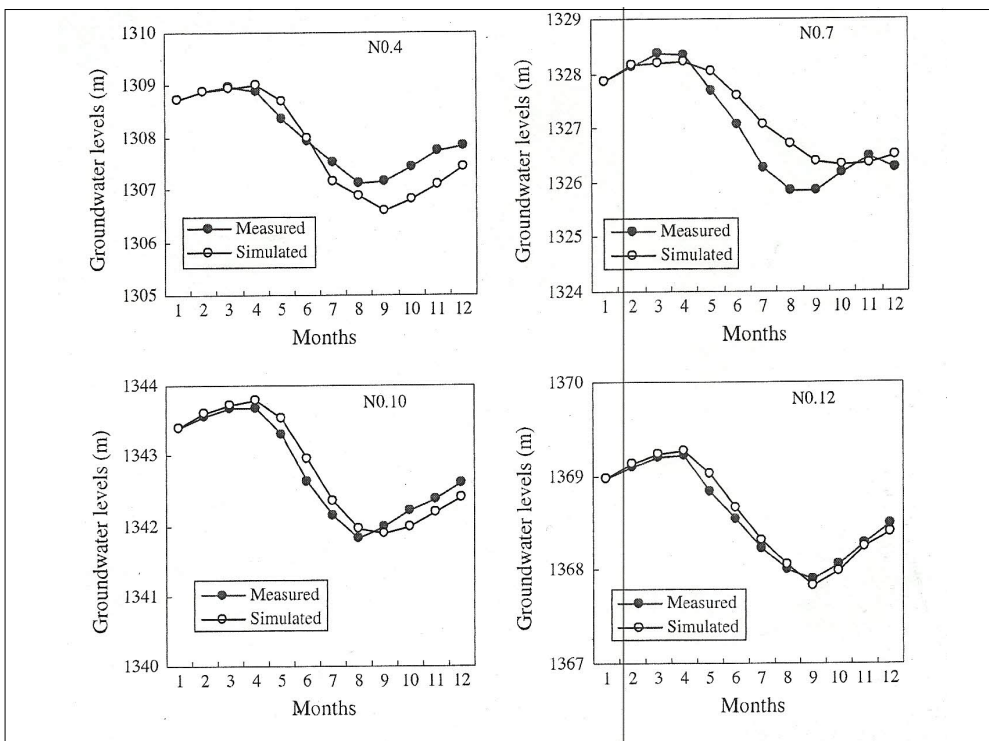


Figure 1: Comparison of simulated and observed groundwater levels for four monitoring wells

Shaoyuan *et al.* (2010) compared simulated and measured groundwater levels from 12 monitoring wells at Minqin oasis in China in 1999. This showed similar groundwater level trends with the hydrogeological situation which indicated that the generalized models of the hydrogeological conditions were reasonable. The models were verified by use of groundwater level data measured in 1999. Figure 1 above shows comparisons between simulated and measured values of groundwater level from four out of 12 monitoring wells in the oasis in 1999. Overall, precision was high for the groundwater with RMSE of 0.71 m, RE of 17.96%, and R2 of 0.84. Overall, the results showed that the trend of changes of simulated groundwater levels basically matched that of the measured values.

Groundwater flow is normally continuous due to hydraulic gradient, pressure gradient or temperature gradient. The flow through the porous medium is governed by the equation of continuity. The velocities in groundwater flow are in general very low; the Reynold's number has generally some value between 1 and 10 for Darcy's law to be valid (Bear, 1988).

The equations governing groundwater flow are partial differential ones (Logan, 1994) whose solutions for non-trivial cases cannot be obtained analytically (Wood, 1993). Fortunately, quite good approximate solutions can be obtained using

computers. In such cases the equations are discretized using methods such as finite differences, finite elements, integrated finite differences, finite volumes and boundary integrals, amongst others. Computer codes can then be developed for the discretized systems of equations and programs written to solve groundwater flow.

In this study, we have developed a model for simulating the effect of pumping out water from several wells in a given idealized aquifer. We have used integrated finite difference method to solve the governing equation. This method is preferred because of the accuracy with which it treats boundaries while maintaining the simplicity differences.

### 1.1 Initial and boundary conditions

Groundwater flow in the aquifer is governed by the boundary conditions of the regional system and the determination of boundary conditions is important for regional groundwater numerical modelling, (Huo *et al.*, 2005). The partial differential elliptic boundary value problem represents the three dimensions in plan aquifer equation for height  $h$  of the water in steady state groundwater flow. This includes second derivatives with reference to the space variables  $x$ ,  $y$ ,  $z$  and it is necessary to have boundary conditions all around the boundary; either known height or known flow. When the groundwater flow is changing with time, the equation representing it becomes parabolic (see equation (2.1)), i.e. it has a first derivative in time and second derivatives in the space coordinates. It is then necessary to have an initial condition as well as boundary conditions all-round the boundary in order to be able to solve our problem represented by the differential equation (2.1) i.e. numerical determination of the hydraulic head distribution within the aquifer as a result of pumping water from some specific points (wells) within the aquifer. The problem is assumed to be well posed, that is the governing equation is formulated so that there is a unique solution and small changes in data make small changes in this solution.

Wood (1993) remarks that to have suitable boundaries, it is often necessary to model a larger area. For this reason we have chosen our model to be an idealized aquifer in form of a rectangular block measuring 3.5 km square with a depth of 10 metres. For the sake of simplicity all the four edges are taken as non-flow boundaries assumed to be bounded by impervious walls. There is therefore no flow into or out of the (confined) aquifer though it must be born in mind that there is actually groundwater movement within the aquifer itself. This is because as stated earlier groundwater is in a continuous flow.

Initially the rate of inflow within the aquifer equals the rate of outflow so that the net velocity is zero. For this reason, initial piezometric height within the aquifer is uniform. In particular the boundary conditions at the four edges are such that the piezometric height is 5 metres. Thus, since in the governing equation, the hydraulic

head,  $h$  is a function of the space coordinates (all restricted to a finite region) and the time  $t$  (unrestricted), we could write  $h(x, y, 0) = 5$  and then proceed to work out  $h(x, y, t)$  subject to  $0 \leq x \leq 3500$ ,  $0 \leq y \leq 3500$ ,  $0 \leq z \leq 10$ ,  $t > 0$ ,  $K > 0$ , the linear measurements being in meters.

The number of blocks, along an edge is chosen odd (in our case 7) in order to have a central block (no.25) through which we can have symmetry either across the aquifer or along its diagonals.

## 2.0 Materials and methods

### 2.1 The governing equation

The governing equation for groundwater flow is the parabolic differential equation in three dimensions given by

$$\nabla^2 h = \frac{S_0}{K} \frac{\partial h}{\partial t} \quad (2.1)$$

$$= \frac{S}{bK} \frac{\partial h}{\partial t} \quad (2.2)$$

$$= \frac{S}{T} \frac{\partial h}{\partial t}, \quad T = bK \quad (2.3)$$

or 
$$T\nabla^2 h = S \frac{\partial h}{\partial t} + Q, \quad Q = \text{net external flow} \quad (2.4)$$

The quantity  $Q$  (Dimensions  $LT^{-1}$ ) represents sinks and sources, or the algebraic sum of extraction flows (pumpage) and replenishment flows (including precipitation, excess irrigation, imported water, stream percolation and artificial recharge).

### 2.2 Discretization of the governing equation

Discretization of a differential equation refers to the process of converting it to discrete components that can be implemented using computer codes (Rice, 1993). This process is necessary for developing a numerical model based on any numerical computing technique. The integrated finite difference method is used to explicitly solve the governing equation. Assuming that the principal components of the hydraulic conductivity, transmissivity and dispersion tensors were aligned in the directions of the Cartesian grid axes, we express equations (2.1) and (2.4) as

$$K_{ij} \frac{\partial^2 h}{\partial x_{ij}^2} = S_0 \frac{\partial h}{\partial t} + Q \quad (2.5)$$

Integrating equation (2.5) over the whole volume since the properties are averaged for each block volume, we obtain:

$$\iiint K_{ij} \frac{\partial^2 h}{\partial x_{ij}^2} dV = \iiint S_0 \frac{\partial h}{\partial t} dV + Q_v \quad (2.6)$$

where  $Q_v$  is summation over volume. However, since we are summing up effects of interaction between block faces, we need to sum over block surfaces instead of block volume. This conversion is done by applying the Gauss divergence theorem to the equation (2.6) above, while assuming that interaction is normal to the block faces. This procedure gives

$$\sum K_{ij} \frac{(h_j^n - h_i^n)}{\Delta x_{ij}} \Delta S_{ij} = V S_0 \left( \frac{h_i^{n+1} - h_i^n}{\Delta t} \right) + Q_v \quad (2.7)$$

where  $V$  is the volume of the block under consideration. The subscript  $i$  refers to the current block,  $1 \leq i \leq 49$  while  $j$  refers to the immediate neighbouring blocks and varies from 1 to 4 depending on the number of block neighbours.  $n$  refers to the current time step while  $n+1$  refers to the next time step. Equation (2.7) can further be rearranged as

$$h_i^{n+1} = h_i^n + \frac{\Delta t}{V S_0} \sum K_{ij} \left( \frac{h_j^n - h_i^n}{\Delta x_{ij}} \right) \Delta S_{ij} - \frac{\Delta t}{V S_0} Q_v \quad (2.8)$$

where  $h_i^{n+1}$  is the hydraulic head we are computing. It is this equation which we have converted into computer codes.

### 2.3 Design of the aquifer

We have considered a model of a confined aquifer of one layer. For the purposes of mathematical calculations of storage and flow of groundwater, we have assumed the aquifer to be homogeneous (hydrologic properties are everywhere identical) and isotropic (hydrologic properties are independent of direction). Moreover, since our aquifer is an idealized one (Lee *et al.*, 1992), we shall take it to be a rectangular block of depth  $b$ . This implies its boundaries are straight. For total independence, the side faces are impervious such that there is no inflow into or outflow from the aquifer. The aquifer is subdivided into 49 identical blocks as illustrated in figure 2 below. Each block measures 500m by 500m by 10m.

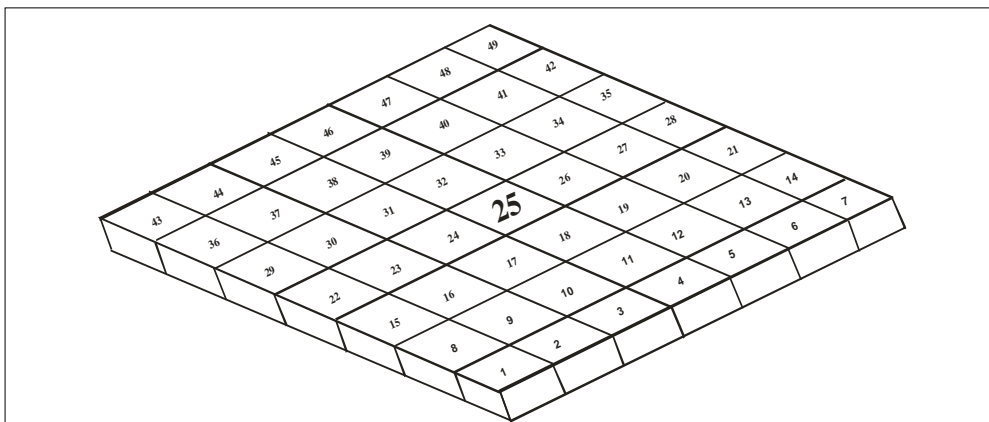


Figure 2.1: Isometric view of an idealized aquifer

The objective of the work is to investigate the variation of the piezometric heights and velocity profiles as time progresses during the pumping process. We have used a time interval of 1.5 days. For the sake of ease in comparison we have considered the wells, drilled in any of the 49 blocks, to be of the same size and the pumping rate to be the same. We have started pumping from the middle block, which is block number 25 (BN25), after which the piezometric heads and velocity profiles in any of the other blocks (BN25 inclusive) can be investigated. Next we pump from the following sets of blocks: {23, 27, 18, 32} and {1, 7, 43, 49}.

### 3.0 Results and discussion

The results of hydraulic heads with respect to time of withdrawal at a constant rate on the two sets of blocks, namely, BN25, BN23, BN27, BN32, BN18 and BN1, BN7, BN43, BN49 are represented in the graphs in figures 3.1a, 3.2a and 3.3a. Now since drawing 49 graphs for each experiment on the same set of axes would lead to too many crowded up graphs on a single page, we have chosen in each case to study the effect of the hydraulic heads and velocity profiles in the middle row only containing block numbers 22, 23, 24, 25, 26, 27 and 28. Thus for each figure there appear seven graphs. Their graphs are found in figures 3.1b, 3.2b and 3.3b respectively.

#### 3.1 Withdrawal on block number 25

In figure 2a, the graphs for the following pairs overlap; 22 and 28, 23 and 27, and 24 and 26. As would be expected, this is due to symmetry with respect to the axis of symmetry passing through block number 25 (BN25). For example (BN22) and (BN28) are three blocks away each from the central block number, (BN25). Consequently, the head loss in BN25 falls drastically to about 3.9 m at the 50<sup>th</sup> day. This is due to the fact that we are pumping directly

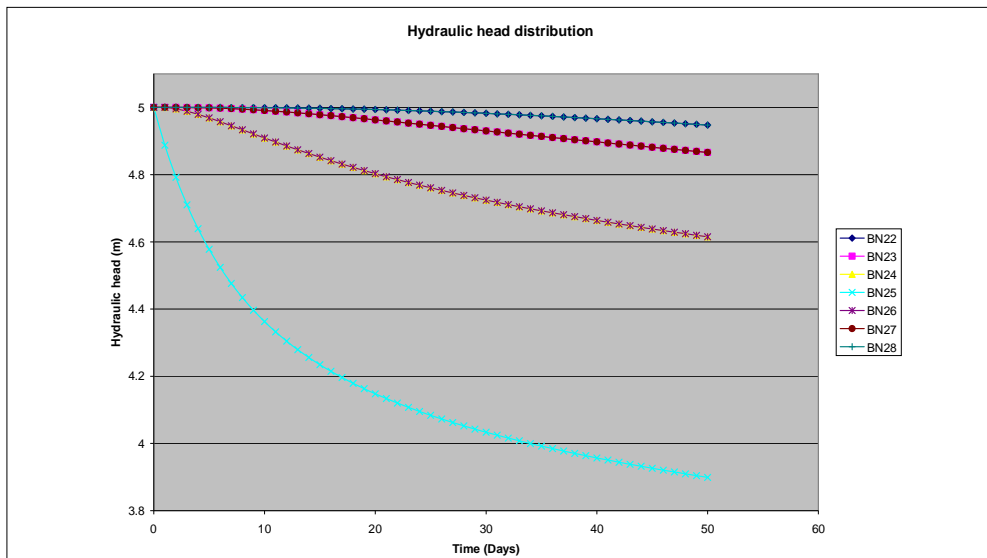


Figure 3.1a: Hydraulic head distribution for withdrawal at a constant rate on block number

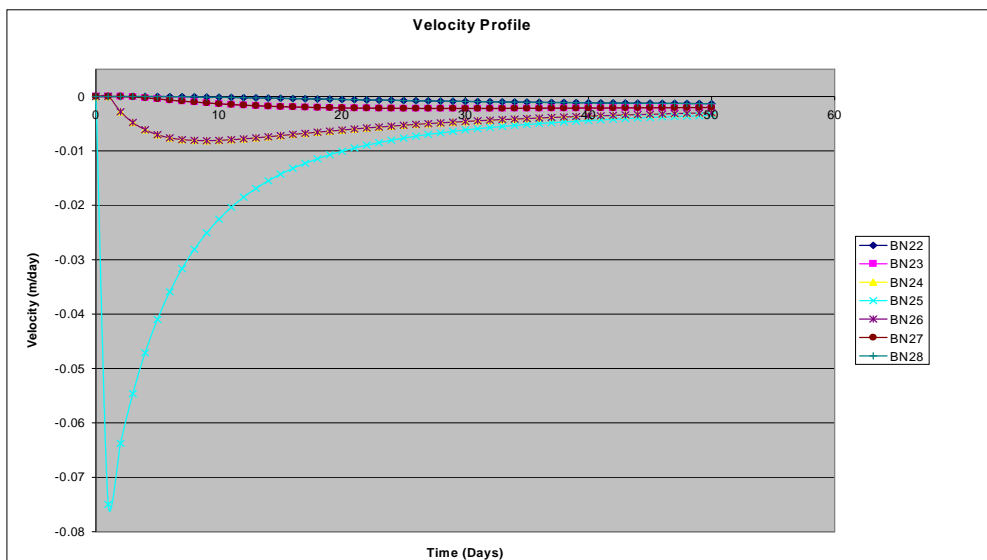


Figure 3.1b: Velocity profiles for withdrawal at constant rate on block number 25

from this block. The velocity for this block drops sharply to approximately -0.075 meters per day as water has to flow faster towards the well due to the great velocity gradient created by the pumpage here. By this reasoning the changes in the hydraulic gradient heads for BN22 and BN28 are least as the blocks are very far from BN25. Similar reasoning explains why the head loss in BN24 and BN26 is more than in BN23 and BN27. As pumping continues the water velocities within the aquifer tend to vanish since the water flow acquires a state of dynamic equilibrium. That is



why the velocity profiles tend to zero after only 50 days. The head loss is greatest in BN23 and BN27 as these are the sources. BN22 and BN28 are affected more than BN24 and BN26 in spite of the two pairs being equidistant from the sources. This is because these two

blocks are bounded on one side by an impervious wall and as such cannot enjoy any replenishment from these walls. On the contrary, BN24 and BN26 can both draw water from BN25, BN32 and BN18, whose equivalence lacks for BN22 and BN28. That is why these pairs of graphs are quite close together. BN25, being farthest from the source, is least affected and for this reason its graph slopes least.

**3.2 Withdrawal on block numbers 23, 27, 32 and 18**

BN23 and BN27 suffer the greatest head losses. This is because; besides being sources they are closest to the impervious boundaries of the aquifer. BN25 is next affected as it is greatly affected by withdrawal on the directly adjacent blocks 18 and 32 apart from being affected, also, by withdrawal on BN23 and BN27 through BN24 and BN26 respectively. BN24 and BN26 are next affected because though directly adjacent to the sources (BN23 and BN27), they are diagonally adjacent to BN18 and BN32. BN22 and BN28 are the least affected because though adjacent to BN23 and BN27 respectively, BN18 and BN32 are too far for their effects to be felt here. Within the first few hours the water velocities towards the wells in BN23 and BN27 are very high (about 0.075 m per day), with their profiles identical with the velocity

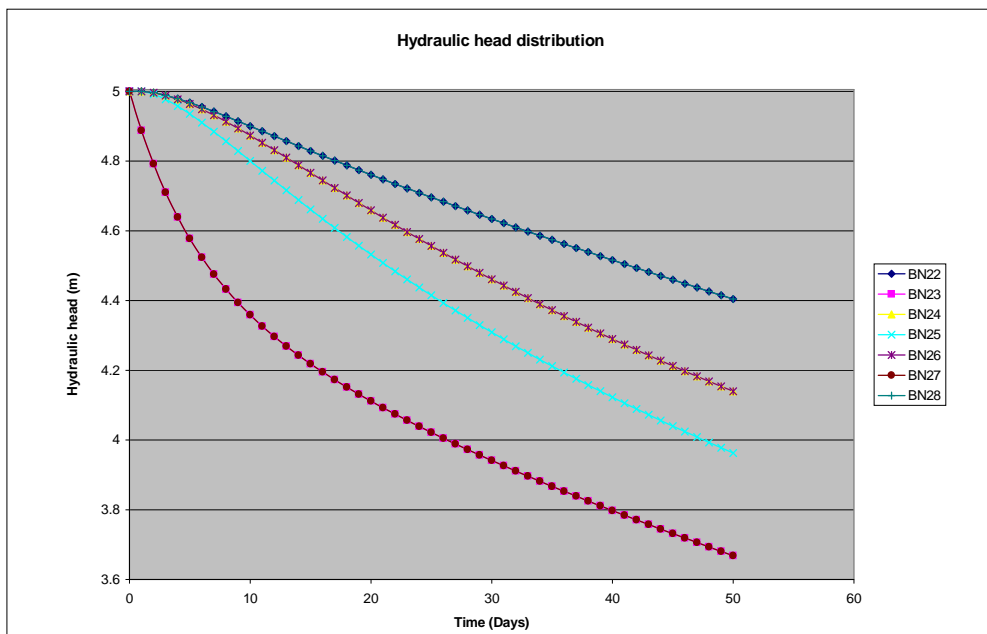


Figure 3.2a: Hydraulic head distribution for withdrawal at a constant rate on block numbers 23, 27, 32 and 18

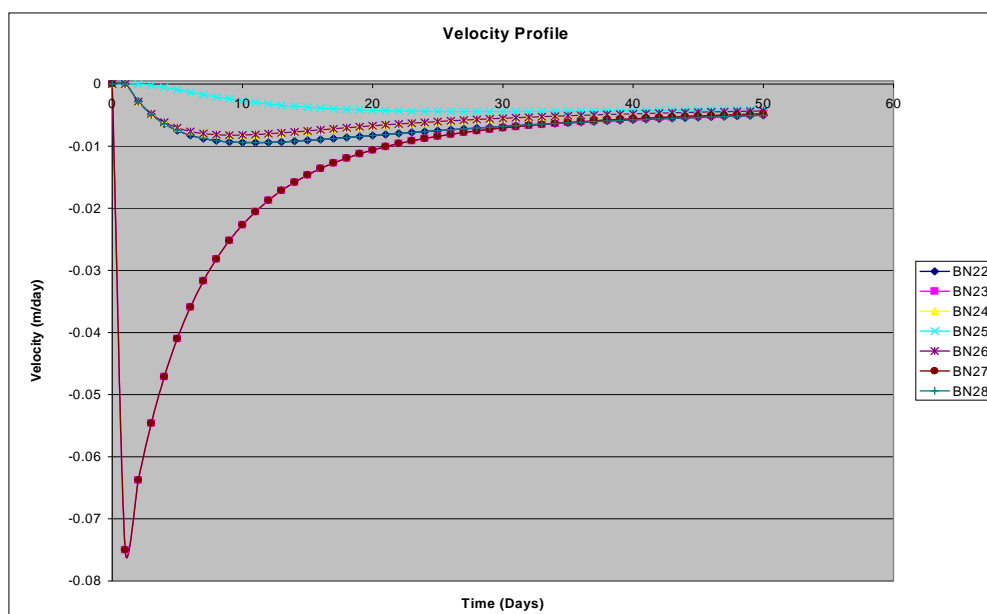


Figure 3.2b: Velocity profiles for withdrawal at a constant rate on block numbers 23, 27, 32 and 18

profile for BN25 in our previous experiment where we were simulating pumpage from BN25 itself. This is because there is pumpage from these two blocks. The velocities in BN25 follow next as water moves to replenish the wells in the directly adjacent blocks 18 and 32. BN22 and BN28 have the least velocity losses due to the fact that apart from being bounded by impervious walls, the water movement is essentially towards BN23 and BN27 only.

#### Withdrawal on corner blocks

BN25, being the farthest from the withdrawal blocks suffers the least hydraulic loss of only 0.004m at the 50th day. By symmetry, BN24 & BN26 follow next, followed by BN23 & BN27. The pair of blocks suffering the greatest head loss is BN22 and BN28 whose piezometric heights stand at only 4.82m at the end of the 50th day. This is because BN22 is closest to withdrawal blocks BN1 and BN43, the same way BN28 is closest to BN7 and BN49.

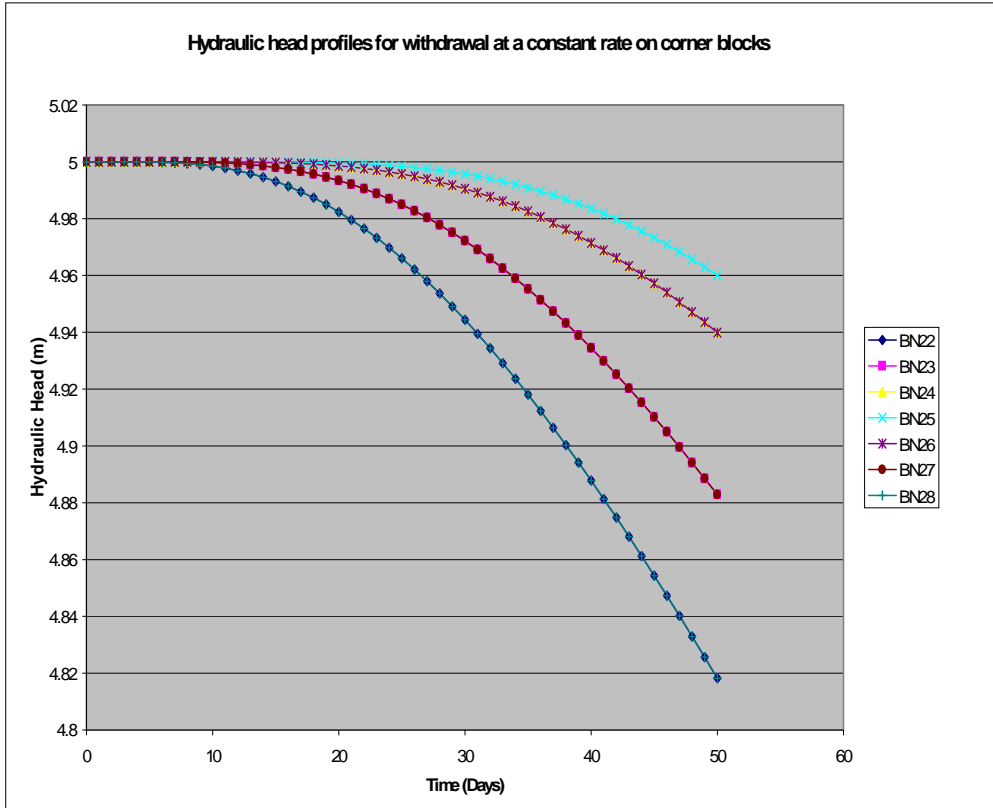


Figure 3.3a: Hydraulic head distribution for withdrawal at a constant rate on block numbers 1,7,43

Incidentally, the head losses in this withdrawal are least compared to the loses in all others experiments as far as the withdrawal effect in the middle row of blocks 22,23,24,25,26,27 and 28 is concerned.

The velocity is least in BN25 due to its great distance from the corner blocks. As would be expected, BN24 and BN26 follow next, followed by BN23 and BN27, the greatest velocities soaring to as high as 0.005m/day being in BN22 & BN28, as these are the closest to the pairs of the corner blocks 1, 43 and 7, 49 respectively.

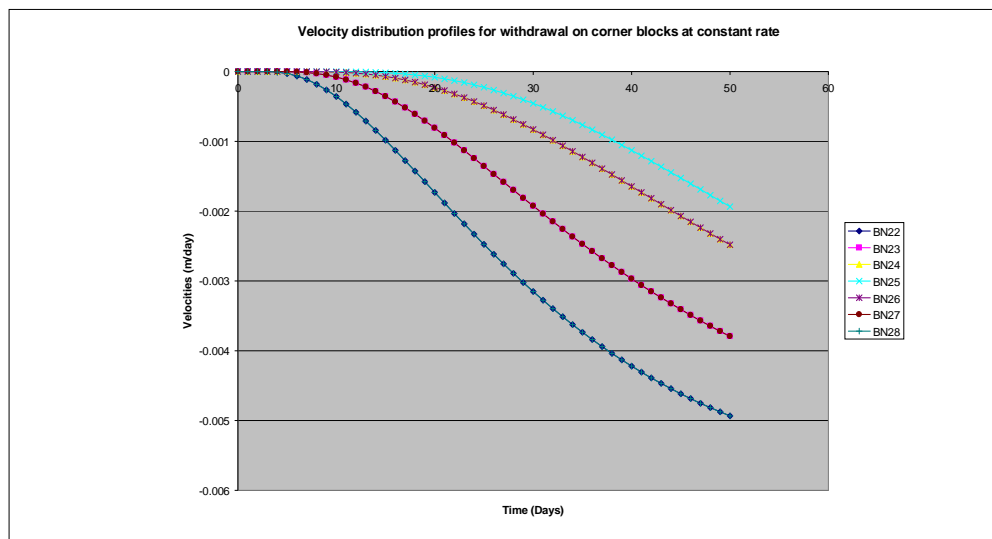


Figure 3.3b: Velocity profiles for withdrawal at a constant rate on block numbers 1,7,43 & 49

#### 4.0 Conclusion

The foregoing results do, however, confirm that the discretized governing equation has successfully generated both hydraulic head and velocity profile distributions. These distributions obtained from the model reveal that there is symmetry in the three sets of withdrawal wells. However, in situations lacking symmetry it would be extremely difficult to accurately predict the results. The results in the few selected cases reveal that the more the number of wells of withdrawal, the greater the loss in the hydraulic heads. For instance, withdrawal from corner blocks leads to the least hydraulic head losses on the middle horizontal row as compared to the rest of the withdrawal blocks. This implies that in practice, the wells ought to be drilled being as far apart as is practically possible, subject to their radii of inference.

Ideally, we would have gone ahead to compare the simulated results with actually measured groundwater levels from an actual discretized aquifer. However, as mentioned there earlier, the cost required would be colossal. However the observations discussions done should suffice to validate the results from this model. These results would guide the aquifer users (through the relevant government institutions) on the number of wells that should be drilled in a given aquifer and at what locations within it. This would be done by limiting the usage of the aquifer to a particular acceptable piezometric level. The model can also be used to simulate the effect of agricultural activities on groundwater levels.

**References**

- Ako B., and Osundu, V. (1986). Electrical resistivity survey of the Kerri-Kerri Formation, Darazo, Nigeria. *Journal of African Earth Services*, **5**, pp.527–534.
- Bear J. (1988). *Dynamics of Fluids in Porous Media*. New York: Courier Dover Publications.
- Davis G. D. (1987). *Numerical Methods in Engineering & Science*. London : Chapman and Hall.
- Evans R., Evans R., Jolly P., Barnet S., Hatton T., Merrick N., (2006, November 9). National Groundwater Reform,. <http://www.ncgm.uts.edu.au/media> .
- Huo Z., Feng S., Kang S., Mao X., and Wang F. (2011). Numerically modelling groundwater in an arid area with ANN-generated dynamic boundary conditions. *Hydrological Processes*, **25** (5), 705-713.
- Lee R., Ketelle R., Rizk J., and Rizk T. (1992, July-August). Aquifer Analysis and Modeling in Fractured Heterogeneous Medium. *National Groundwater Association*, **30** (4), pp. 589-597.
- Logan, T. D. (1994). *An Introduction to Linear Partial Differential Equations*. New York: John Wiley & Sons.
- Matej, G., Wemaere, I., & Jan, M. (2007). Regional groundwater model of North-East Belgium. *Journal of Hydrology*, **335** (1-2), pp. 133–139.
- Napier T. L., Scott D., Easter K. W., and Supalla R. (Eds.). (1983). Water resources research. Problems and potentials for agriculture and rural communities. 1983 pp. xii + 247pp. *Problems and Potential for Agriculture and Rural Communities*, 247.
- Raudkivi R. A., and Callander A. J. (1976). , *Analysis of Groundwater Flow*. London: Edward Arnold.
- Rice J. R. ( 1993). *Numerical Methods: Software and Analysis*. San Diego : Academic Press, Inc.
- Shaoyuan F., Huo Z., and Kang S. (2010, May 5). Groundwater simulation using a numerical model under different water resources management scenarios in an arid region of China. *Environ Earth Sci* .
- The Environment Agency | enquiries@environment-agency.gov.uk. (2012, May 22). Groundwater Protection Policy and Practice. *Environment Agency* .
- Wood, W. (1993). *Introduction to Numerical Methods for Water Resources*. New York: Oxford University Press.
- Zhao C., Wan Y., Xi C., and B. G., L. (2005). Simulation of the effects of groundwater level on vegetation change by combining FEFLOW software. *Ecological Modelling*, pp.341–351.